Rotating Bose Einstein Condensates

Ponnuraj Krishnakumar

December 14, 2011

Abstract

This paper contains a review of dilute Bose-Einstein gas, both in a box and in a harmonic trap, and when they form condensates. As the Bose-Einstein condensate (BEC) begins to rotate vortices begin to appear and their dynamics are studied. For more rapid rotation, the vortices begin to form regular arrays and for very high rotation rates, one begins to see Landau levels. Eventually as the rotation rate approaches the radial trap frequency, there is an expected quantum phase transition to a highly correlated state analogous to those found in fractional quantum hall effect for electrons in a strong external magnetic field.

1. Introduction

The outline and format of this paper closely follows the review paper by A. Fetter [1]. Any and all details may be found in this review and the references included in the review. Section 2 of this paper begins with a recap of BEC in an ideal bose gas both in a box as well as in a harmonic trap. The effects of interactions are also studied. The effects a few vortices in a rotating BEC are considered and their stability at different rotation rates are analyzed in section 3. Section 4 deals with vortex arrays in the Thomas-Fermi (TF) regime. Various aspects of rotation rates on the vortex arrays are studied and corresponding experimental results are provided where available. The next section discusses the lowest Landau level (LLL) regime and the transition to a highly correlated state at extremely high rotation rates. The last section contains a brief summary and the conclusion.

2. Physics of BEC in dilute trapped gases

2.1 Ideal Bose Gas

Let us first consider an ideal Bose gas in an external trap potential V_{tr} with a complete set of single particle energies ϵ_j. The mean occupation of a specific state is given by the familiar expression $n_j = (e^{\beta(\epsilon_j - \mu)})^{-1}$. The classical regime corresponds to the situation where $n\lambda_T^3 \ll 1$, where n is the mean density of particles and $\lambda_T = h/\sqrt{Mk_BT}$ is the thermal wavelength. In this regime the chemical potential μ is large and negative. As the temperature decreases or equivalently the density increases, μ grows. The onset of BEC at some critical temperature T_c is given by the relation $\mu(T_c, N) = \epsilon_0$, where ϵ_0 is the ground state energy in the potential V_{tr}. Below T_c, μ is fixed at this value and the ground state is characterized by a macroscopic occupation. The number of particles not in the condensate $N^{'}(T)$ is given by

$$N^{'}(T) = \int d\epsilon \frac{g(\epsilon)}{e^{\beta(\epsilon-\epsilon_0)} - 1} \tag{1}$$

The total number of particles is then given as $N = N_0(T) + N^{'}(T)$.

Let us now consider two specific situations when the BEC is in a box with periodic boundary conditions and when it is placed in a harmonic trap.

When the ideal BEC is placed in a box with periodic boundary conditions

(say a box of volume V), the single particle eigenstates are simply plane waves (i.e. $\psi_k(r) \approx e^{ik.r}$) with energies $\epsilon_k = \hbar^2 k^2/(2M)$. Here $k_i = 2\pi n_i/L$ is quantized along each of the directions with n_i an integer and the lowest energy state is $\epsilon_0 = 0$. The density of states $g(\epsilon)$ is

$$g(\epsilon) = \frac{V}{4\pi^2}(\frac{2M}{\hbar^2})^{3/2}\epsilon^{1/2} \tag{2}$$

For $T < T_c$ one can show that

$$\frac{N_0(T)}{N} = 1 - \left(\frac{T}{T_c}\right)^{3/2} \tag{3}$$

Note that the above result can be generalized to any dimension d for $d > 2$. However, the integral in (1) diverges for $d \leq 2$. Hence a uniform gas cannot from a BEC in one or two dimensions.

Now consider a BEC in an external anisotropic harmonic trap of the form

$$V_{tr}(r) = \frac{1}{2}M(\omega_x^2 x^2 + \omega_y^2 y^2 + \omega_z^2 z^2) \tag{4}$$

The single particle energies are given as $\epsilon = \hbar(n_x\omega_x + n_y\omega_y + n_z\omega_z) + \epsilon_0$, where n_i are nonnegative integers and $\epsilon_0 = \frac{1}{2}\hbar(\omega_x + \omega_y + \omega_z)$ is the zero point energy. The corresponding density of states is

$$g(\epsilon) = \frac{\epsilon^2}{2\hbar^3\omega_0^3} \tag{5}$$

where $\omega_0^3 = \omega_x\omega_y\omega_z$ defines a geometric mean trap frequency. Once again BEC in the harmonic trap occurs when $\mu = \epsilon_0$ and the following temperature dependent equation can be obtained.

$$\frac{N_0(T)}{N} = 1 - \left(\frac{T}{T_c}\right)^{3} \tag{6}$$

Note that the BEC in a harmonic trap does not have a divergence in (1) for $d = 2$. This implies that the two dimensional bose gas in a harmonic trap can form a BEC with a finite transition temperature T_c. This is a major difference between a BEC in a harmonic trap compared to a BEC in a box. The rest of this paper focuses on BEC in a trap.

2.2 Effects of interparticle interactions

The Gross-Pitaevskii (GP) energy functional for a BEC in a trap with confining potential V_{tr} is given by

$$E_{GP}[\Psi] = \int dV \left(\frac{\hbar^2 |\nabla \Psi|^2}{2M} + V_{tr} |\Psi|^2 + \frac{1}{2} g |\Psi|^4 \right) \tag{7}$$

Here Ψ represents the macroscopic condensate wave function. The first two terms in the above expression are the kinetic energy and the trap potential respectively. The last (quartic) term describes the effect of interactions. Comparison of the kinetic and trap energies yields the oscillator length $d_0 = \sqrt{\hbar/M\omega_0}$ which characterizes the mean size of the non-interacting condensate. Similarly a comparison between the kinetic and interaction energies yields the healing length $\xi = \hbar/\sqrt{2Mgn}$ which characterizes the length scale over which the condensate heals back to its uniform value n (the condensate density). Bogoliubov noticed that the repulsive interparticle interactions can be characterized by a positive s-wave scattering length a, which is typically a few nanometers for dilute alkali metals of interest. This along with d_0, yields a new dimensionless parameter Na/d_0 which acts a measure of how important the interactions are. In the usual situation, this parameter is large resulting in the regime known as Thomas-Fermi (TF) limit. In this case the repulsive interactions dominate and the mean radius R_0 greatly exceeds the mean oscillator length d_0 making the kinetic energy negligible. Dropping the kinetic energy term from (7) and minimizing with respect to $|\Psi|^2$, we get the TF approximation (which is a special case of the general GP equation)

$$V_{tr} + g|\Psi(r)|^2 = \mu \tag{8}$$

Using the expression for the trap potential discussed above one can derive the relation $d_0 = \sqrt{\xi R_0}$. Here $R_0^3 = R_x R_y R_z$ and R_i are the condensate radii along different directions. This also yields a clear separation between the length scales in the TF limit $\xi \ll d_0 \ll R_0$.

One can also consider the general time-dependent GP equation

$$i\hbar \frac{\partial \Psi(r,t)}{\partial t} = \left[-\frac{\hbar^2 \nabla^2}{2M} + V_{tr}(r) + g|\Psi(r,t)|^2 \right] \Psi(r,t) \tag{9}$$

Assuming a stationary nonuniform condensate wavefunction and considering small perturbations around this state, one can compute the spectrum

$$E_k = \left[\frac{gn\hbar^2 k^2}{M} + \left(\frac{\hbar^2 k^2}{2M} \right)^2 \right]^{1/2} \tag{10}$$

where n is the condensate density and $\mu \approx gn$ for the uniform gas. In the long wavelength limit ($k\xi \ll 1$), the spectrum reduces to the familiar phonon spectrum $E_k \approx \hbar s k$ where $s = \sqrt{gn/M}$ is the speed of compressional sound. In the opposite case when $k\xi \gg 1$ the spectrum becomes a free particle spectrum. This expression is similar to the quasiparticle spectrum predicted by Landau for superfluid Helium. In the case of superfluid helium there exists a critical velocity above which dissipation occurs. For the above spectrum $v_c = s$. Note that as $s = \sqrt{gn/M}$, this implies that s exists only because $g > 0$ i.e. the interactions are repulsive. This means that an ideal Bose gas ($g = 0$) can never be a superfluid even at $T = 0$ even though a $k = 0$ condensate is present. Thus the occurrence of superfluidity in a uniform dilute bose gas is purely due to the presence of repulsive interactions.

3. Physics of few vortices in a trap

The local velocity field can be expressed as $v = \nabla\Phi$ where Φ is proportional to the phase of the macroscopic condensate wave function. This along with the single valuedness of the wavefunction can be used to show that any circulation in a dilute BEC must be quantized in units of $2\pi\hbar/M$. The important point here is that results of vortex dynamics in an irrotational fluid may be carried over to a dilute BEC. However, for a BEC in a trap, the nonuniformity of the density severely affects the vortex dynamics.

A classical viscous fluid in a container that rotates with angular velocity Ω, also acquires the same velocity. Consider a static Hamiltonian $H(r, p)$ with a trap potential. A transformation to the laboratory frame gives

$$H^{'}(r^{'}, p^{'}) = H(r^{'}, p^{'}) - \Omega \cdot L(r^{'}, p') \tag{11}$$

where the primed coordinates and primed terms represent quantities in the rotating frame. This yields the modified GP equation written in the

rotating frame

$$E'[\Psi] = \int dV \left[\frac{\hbar^2}{2M} |\nabla \Psi(r)|^2 + V_{tr}(r)|\Psi(r)|^2 + \frac{1}{2} g |\Psi(r)|^4 - \Omega \cdot \Psi^*(r) \mathbf{r} \times \mathbf{p} \Psi(r) \right] \tag{12}$$

Note that the last term favors states with nonzero (positive) Ω. The following analysis is performed in the TF limit where $\xi \ll d_0 \ll R_0$. In the presence of vortices, ξ also corresponds to the vortex core size. The presence of a few vortices does not affect the number density significantly.

One can compute the stability of a vortex for different rotation rates Ω. The regimes depend on a quantity Ω_c which is interpreted as the thermodynamic critical angular velocity for the creation of a singly quantized vortex in the TF limit. Define $\Omega_m = \frac{3}{5}\Omega_c$. When $\Omega < \Omega_m$, the vortex state is unstable and it moves away from the center until it spirals out of the edge. For $\Omega_m < \Omega < \Omega_c$, the vortex state is locally stable near the center of the trap but not globally. Finally for $\Omega > \Omega_c$, the central vortex is both locally and globally stable.

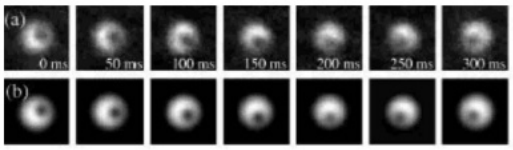

Figure 1: Precession of vortex in a trapped BEC. From [2]

One may also study the dynamics of a trapped vortex by studying the time-dependent GP equation. Applying this to a single straight vortex in a disk shaped condensate produces a solution with an angular precession of a trapped vortex. This is shown experimentally in Fig. 1.

4. Vortex arrays in mean-field TF regime

Consider an incompressible fluid with velocity $v(r)$ in a container rotating with angular velocity Ω. The relevant energy terms are

$$E' = \int dV \left(\frac{1}{2} M v^2 - M \Omega \cdot r \times v \right) n \tag{13}$$

where $n(r)$ is the number density. Re-expressing the above equation one can show show that the absolute minimum of $E^{'}$ is when $v = \Omega \times r$. By using energy arguments and the quantization of vortices in a superfluid, one gets

$$n_v = \frac{M\Omega}{\pi\hbar} \tag{14}$$

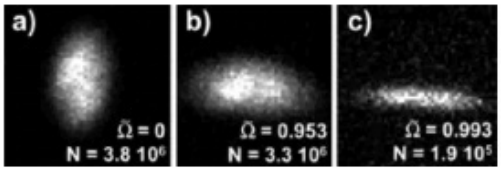

Figure 2: Sideview of BEC in a trap. As the rotation rate increases the axial direction is severely compressed and the radial direction expands. From [3]

This shows that an increase in the rotation rate also increases the vortex density n_v. The above relation holds strictly for a superfluid in a rotating bucket. When put in a harmonic trap, one has to consider corrections due to centrifugal forces which expand the condensate radially and shrinks it along the rotation axis. As a result the total number of vortices increases at a rate faster than linearly with Ω. To quantify this dependence is rather detailed. The final result in the TF limit is

$$\frac{R_\perp(\Omega)}{R_0(0)} = \left(1 - \frac{\Omega^2}{\omega_\perp^2}\right)^{-3/10}, \frac{R_z(\Omega)}{R_z(0)} = \left(1 - \frac{\Omega^2}{\omega_\perp^2}\right)^{1/5} \tag{15}$$

Here the sublabels $\perp$ and z refer to the direction perpendicular and parallel to the axis of rotation Ω respectively. $\omega_\perp$ is the frequency of the trap in the radial direction. As mentioned earlier the condensate expands radially and shrinks axially as Ω is increased approaching a two-dimensional configuration. The below ratio acts as a tool to determine the actual angular velocity. Fig. 2 shows some experimental data.

$$\frac{R_z(\Omega)}{R_\perp(\Omega)} = \frac{\sqrt{\omega_\perp^2 - \Omega^2}}{\omega_z} \tag{16}$$

Also the chemical potential can be computed to be

$$\mu_{TF}(\Omega) = \mu_{TF}(0)(1 - \Omega^2/\omega_\perp^2)^{2/5} \tag{17}$$

This shows that the chemical potential decreases continuously and vanishes as $\Omega \to \omega_\perp$ indicating a lack of radial confinement for high rotation rates.

These rapidly rotating condensates also tend to form dense arrays of vortices. Fig. 3 shows experimental evidence of highly uniform triangular vortex lattices that closely resemble those of Abrikosov lattices in type II superconductors.

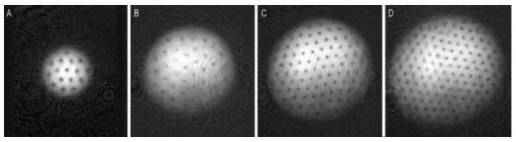

Figure 3: Observation of vortex lattices. From reference [4]

The effects of rapid rotation on the condensate were discussed above. Another aspect is its effects on the vortex core radius ξ. Define l to be the radius of the cell and $\overline{\Omega} = \Omega/\omega_\perp$. It was found that for small and moderate $\overline{\Omega}$, $r_{core} \approx \xi$. As $\overline{\Omega} \to 1$, the ratio r_{core}^2/l^2 saturates at a value $\frac{1}{2}$. Fig. 4 shows experimental and numerical values (See references in [1]). For small values of Ω, $\xi^2 \propto \Omega$ in the TF limit. As Ω rises to the critical value $\omega_\perp$ the core area saturates to a constant value.

Now let us turn to the vortex array. Tkachenko showed that the triangular lattice has the lowest energy (for lattices with one vortex per unit cell). This was also seen earlier in Fig. 3. Further, he also determined the small-amplitude normal modes of a vortex lattice, along with the corresponding eigenvectors for a given wave vector k lying in the x-y plane perpendicular to Ω. The result for long wavelengths ($kl \ll 1$), where $l = \sqrt{\hbar/M\Omega}$ is the vortex cell-radius, is a primarily transverse wave with linear dispersion $\omega(k) \approx c_T k$, where $c_T = \frac{1}{2} l\Omega$ is the transverse propagation speed. This is essentially a long wavelength photon in the vortex lattice. Recall that rapidly rotating BEC are axially compressed making them more two dimensional. This work of Tkachenko was

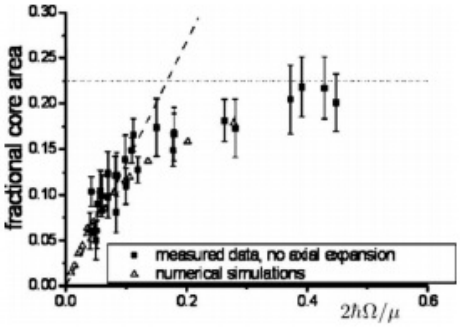

Figure 4: Vortex core area as a function of rotation rate. For higher rotation rates the vortex core area appears to saturate to some constant value. From reference [5]

generalized to find the following long-wavelength dispersion

$$\omega(k)^2 \approx c_T^2 k^2 \frac{s^2 k^2}{4\Omega^2 + s^2 k^2} \tag{18}$$

where s is the speed of sound. These Tkachenko oscillations were observed in considerable detail (Fig. 5 which shows the image of the resultant distorted lattice). The lines in the figure are a sine fit and indicate the distortion of the lattice. Though the normal mode has the right shape, the measured frequency is less compared to (18).

As seen earlier, in the mean-field TF regime, for a harmonic trap with radial frequency $\Omega > \omega_\perp$ the system cannot be confined. It is thus useful to consider the effects of adding a stronger confining potential like r^4. Such a trap will confine the system even for frequencies above $\omega_\perp$ giving rise to new states. The result is

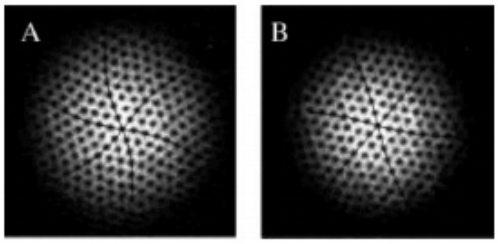

Figure 5: Lowest Tkachenko mode of the vortex lattice. From reference [6]

$$g|\Psi(r)|^2 = \mu + \frac{1}{2}[(\Omega^2 - 1)r^2 - \lambda r^4] \tag{19}$$

Once again μ decreases as Ω increases. Further for a critical value $\Omega_h > 1$, the chemical potential can vanish when the central density is also zero. This indicates the formation of a central hole. For rotation rates above Ω_h, $\mu < 0$ and the condensate assumes an annular form. As Ω further increases, there is a possible second transition to a purely irrotational (vortex-free) state known as a 'giant vortex'. These effects were studied experimentally in Fig. 6 which shows the vortex array for various rotation speeds. Initially, one can see a regular vortex array. Beyond a certain frequency, the array appears irregular and a local minimum in the density can be seen near the center in Fig. 6 d), e) and f). The last two figures i.e Fig. 6 g) and h) are puzzling. In Fig. 6 g) there is an absence of visible vortices whereas in Fig. 6 h) the condensate collapses, the reason for which is still unknown.

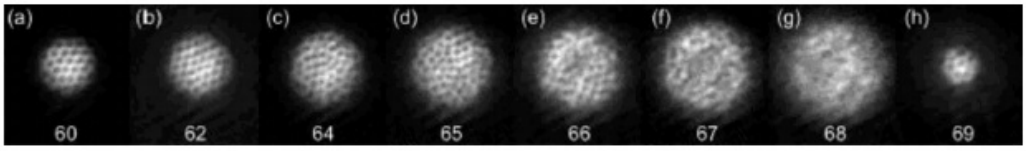

Figure 6: Pictures of rotating gas taken along rotation axis. From [7]

5. Vortex arrays in mean-field LLL regime

The basic assumption of the mean-field TF description was the neglect of the kinetic energy associated with density variations as the vortex cores are small. As the rotation frequency increase, the vortex cores become comparable to the intervortex separation and the above assumption is no longer valid. In this regime the condensate becomes two-dimensional and the interaction energy per particle is small. Neglecting the interaction makes the Hamiltonian quadratic and exactly solvable.

Let us begin by considering a simpler problem, one of a two-dimensional harmonic oscillator (nonrotating). The motion of the oscillator corresponds to that of a two independent oscillators (along x and y) giving rise to circular motion with frequency $\omega_\perp$. When viewed in a frame rotating with frequency Ω, we get $\omega_\pm = \omega_\perp \mp \Omega$. A more appropriate quantum mechanical description involves using creation and annihilation operators and for convenience circularly polarized states, $a_\pm$ and $a_\pm^+$, are used. Expressing the Hamiltonian in term of these operators, it is easy to compute the energy eigenvalues $\epsilon(n_+, n_-) = n_+\hbar(\omega_\perp - \Omega) + n_-\hbar(\omega_\perp + \Omega)$ where n_+ and n_- are integers. For rapid rotation rates as $\Omega \to \omega_\perp$, the important contribution to ϵ is from the n_- term and n_- becomes the Landau level index with the different landau levels separated by $\approx 2\hbar\omega_\perp$. These lowest Landau level (LLL) wave functions appear in fractional quantum hall effect for two dimensional electrons in a strong magnetic field. Hence this regime is referred to as the quantum hall regime.

The LLL regime is valid when $1 - Z/2N\tilde{a} \leq \overline{\Omega}$ where $\tilde{a}$ is the renormalized scattering length. In experiments $\overline{\Omega} \geq 0.99$ to reach this regime. The mean-field LLL regime has a BEC with macroscopic occupation and is a superfluid. For even higher $\overline{\Omega}$, there is another quantum phase transition to a highly correlated ground state Ψ_{corr}.

Consider the ratio $\nu = N/N_v$ (where N_v is the number of vortices) which is known as the filling factor in analogy with a similar quantity in the quantum hall effect. Numerous studies show that the GP vortex lattice is the ground state for $\nu_c \approx 6 - 10$ where the specific value depends on the number of vortices and geometry of the system. Vortex lattices are stable for $\nu > \nu_c$. This is a ground state that breaks rotational symmetry. On the other hand for $\nu < \nu_c$, the ground states are rotationally symmetric incompressible vortex liquids that are eigenstates of L_z. These states have close analogies to the fractional quantum hall states for a two dimensional electron gas in a strong magnetic field. The simplest of these many body states is the bosonic Laughlin state. Let us point out some of the crucial differences between these Laughlin type states and the GP states we saw earlier. Firstly, the Laughlin state has a product factor which implies the absence of off-diagonal long range order and hence no BEC. The Laughlin state also vanishes whenever two particles are at the same location. In contrast the GP ground state has all the particles in a single ψ_{LLL} state.

To qualitatively understand the nature of the transition consider N bosonic particles in a two dimensional plane (resulting in $2N$ degrees of freedom). Vortices appear when the system rotates. These vortices have N_v collective degrees of freedom and tend to reduce the overall degrees of freedom to $2N - N_v$. When the system is rotating slowly the $2N$ degrees of freedom of the bosonic particles sufficiently describe the system as $N_v \ll N$. However, when N_v is comparable to N, there is a significant reduction in the overall degrees of freedom resulting in a transition to a completely different state. There are several proposals to study these states experimentally. More detailed references can be found in [1].

6. Summary and Conclusion

For slow rotation rates ($\overline{\Omega} = \Omega/\omega_\perp << 1$), the condensate only has a few vortices. The overall density profile can be well described using that of a nonrotating condensate apart from the vortex cores. Experiments have been able to study the dynamics of vortices in such systems. See review [1] for references to experimental studies. As the rotation rate increases, the centrifugal forces cause the condensate to distort. For $\overline{\Omega}$ (typically $0.75 \leq \overline{\Omega} \leq 0.99$) not too large, the intervortex spacing $\approx l = \sqrt{\hbar/M\Omega}$ is large compared to ξ, the vortex core size. This is the Thomas-Fermi (TF) regime where the kinetic energy term is negligible. For very large rotation speeds

$(0.99 \leq \overline{\Omega} \leq 0.999)$, the vortex cores begin to expand. Hence l is no longer large compared to ξ. Here the interaction energy can be neglected. This is mean-field lowest-Landau level (LLL) regime and is the rotational analog of the landau levels for an electron in an uniform magnetic field. These degenerate landau levels are separated by an energy gap $\approx 2\hbar\omega_p$. Here the LLL states provide a convenient description. Finally for $\overline{\Omega} \geq 0.999$, there is a quantum phase transition to a highly correlated state. The exact nature of these states and the complicated phase transitions in this regime are still under debate.

This term paper contains a very brief overview of rotating BEC, formation and role of vortices at different rotation rates. There are many remarkable experiments and several theoretical predictions (only some of which are mention here), many of which still need to be verified experimentally.

References

[1] A. L. Fetter, Rev. Mod. Phys. **81**, 647 (2009).

[2] Anderson. B. P., P. C. Haljan, C. E. Wieman and E. A. Cornell, Phys. Rev. Lett. **85**, 2857 (2000).

[3] Schweikhard. V., I. Coddington, P. Engels, V. P. Mogendorff and E. A. Cornell, Phys. Rev. Lett. **92**, 040404 (2004).

[4] Abo-Shaeer. J. R, C. Raman, J. M. Vogels and W. Ketterle, Science **292**, 476 (2001).

[5] Coddingtion. I, P. C. Haljan, P. Engels, V. Schweikhard, S. Tung and E. A. Cornell, Phys. Rev. A **70**, 063607 (2004).

[6] Coddingtion. I, P. Engels, V. Schweikhard and E. A. Cornell, Phys. Rev. Lett. **91**, 100402 (2003).

[7] Bretin. V., S. Stock, Y. Seurin and J. Dalibard, Phys. Rev. Lett. **92**, 050403 (2004).